Proceedings of the 21st ICSMGE, Vienna, Austria, 14 – 19 June 2026. Pistrol, Adam & Schweiger (eds.)
Published by: ÖGG, Austrian Society for Geomechanics, Salzburg, Austria, ISBN 978-3-9503898-4-5
https://doi.org/10.53243/ICSMGE2026-1095

Investigation of seismic signature induced by grain-bed impact to determine the grain size distribution of fall-type granular geohazards

Yihan Wang, Clarence Edward Choi
The Department of Civil Engineering, The University of Hong Kong, HKSAR, China, cechoi@hku.hk

Xinzhi Zhou, Yifei Cui
State Key Laboratory of Hydroscience and Engineering, Tsinghua University, Beijing, China

ABSTRACT: Granular geohazards can include grains with diameters from microns to meters. The grain size distribution (GSD) of the composition significantly affects its mobility and erosive properties, making GSD a critical factor for understanding granular geohazards. While the characteristic grain diameter can provide some insight into the GSD, the actual GSD of granular geohazards can vary considerably. Furthermore, traditional techniques for measuring GSD cannot holistically describe the dynamic GSD of a flow. Thus, there is a clear need for more effective tools to enhance current methodologies. Recent advancements in seismic sensing have proven to be valuable for characterizing geohazards. Integrating experimental methods and analytical theory, our study aims to elucidate the relationship between GSD and the seismic signatures generated by grain-bed impacts, with the goal of developing a new seismic impact model that incorporates GSD. A newly developed free-fall experimental apparatus has been employed to conduct both single-grain and dual-grain falling tests as unit tests. Building upon the findings from these unit tests, we carried out multi-grain experiments with varying GSDs to analyze the relationship between GSD and seismic signatures. Single-grain impacts shows that the centroid frequency (f_{mean}), elastic energy (W_{el}), and total power spectral density (PSD_T) of the seismic signal scale proportionally with $d^{-0.5}$, d^5, d^3, respectively. Comparative analysis of different GSDs reveals that conventional metrics proposed in the literature (d_{30}, d_{50}, and d_{94}) exhibit limited correlations with seismic signal characteristics. In contrast, the newly proposed GSD parameter GSD_e, which incorporates fractal dimension (D_f), shows unique correlations with f_{mean}, W_{el}, and PSD_T. Ultimately, a newly-modified seismic impact model considering GSD has been proposed for granular geohazards. This study offers significant insights for practitioners by leveraging seismic signals to elucidate the characteristics of granular geohazards.

KEYWORDS: Grain size distribution; seismic signal; laboratory tests; geohazard mitigation; fractal behavior.

1 INTRODUCTION

Granular geomaterials in free-fall under gravitational influence, including rockfalls (Roy et al., 2019) and debris flows (Iverson et al., 1997), present significant hazards to both human populations and infrastructure in mountainous regions worldwide. A thorough understanding of the composition and dynamics of these granular flows is essential for accurate hazard assessment and the formulation of effective mitigation strategies. In recent years, considerable research efforts have focused on advancing real-time monitoring and early-warning systems to reduce geological risks (Dammeier et al., 2011; Saló et al., 2018). Predictive analysis of granular geohazards using real-time monitoring data has proven to be an effective method for obtaining critical hazard information, facilitating timely risk management and disaster prevention measures (Schimmel et al., 2016).

Previous studies have identified strong correlations between seismic signals and key flow parameters, including total volume (Farin et al., 2015), flow depth (Hu et al., 2018), and flow composition (Haas et al., 2021). However, one critical yet understudied aspect is the relationship between seismic signals and grain size distribution (GSD), which has been shown to significantly influence flow mobility (Song & Choi, 2021). Real-time monitoring of GSD in granular geohazards remains particularly challenging. Conventional approaches typically depend on post-event deposit analysis (Kim & Lowe, 2004), which often fails to capture transient but crucial dynamic processes occurring during mass movement.

Recent research has attempted to characterize granular assemblies of varying sizes using a single effective grain diameter. For instance, Barrière et al. (2015) and Wyss et al. (2016) conducted flume experiments to establish empirical relationships between seismic vibration amplitudes, frequency components, and the median grain diameter (d_{50}) of granular assemblies. However, Haas et al. (2021) demonstrated that different effective grain diameters produce distinct seismic signatures, suggesting that a single representative diameter is insufficient to fully describe the relationship between seismic signals and GSD. Consequently, further investigation is required to elucidate the fundamental connections between GSD and seismic signatures.

To advance this understanding, it is necessary to refine physical seismic models and validate them with experimental data. Existing studies have employed laboratory-scale experiments, including flume tests (Hu et al., 2018; Farin et al., 2019a) and free-fall impact tests (Farin et al., 2015; Lin et al., 2022; Li et al., 2024), to examine the high-frequency seismic response of granular geohazards. In this study, we conduct free-fall impact experiments involving single-grain, dual-grain, and multi-grain tests with controlled grain size distributions to systematically quantify the relationship between seismic signal characteristics and GSD.

2 FREE-FALL EXPERIMENTS

The experimental setup, illustrated in Figure 1 (a), comprises a free-fall apparatus featuring a rigid frame equipped with a hopper and a pneumatically actuated release mechanism for controlled grain deployment. The impact surface consisted of a 500 × 500 × 10 mm polymethyl methacrylate (PMMA) plate (Young's modulus = 3 GPa). A high-speed digital camera (acquisition rate: 1000 frames per second; resolution: 976 × 1064 pixels) was positioned orthogonally to the impact plane to document the collision dynamics.

Figure 1 (b) presents the instrumentation configuration in plan view. Three integrated electronics piezoelectric (IEPE) accelerometers (frequency response: 1 Hz - 20 kHz) were mounted at radial distances of 100, 200, and 300 mm from the plate center to record seismic signals. Simultaneously, four precision load cells (CLS-1KN, Tokyo Measuring Instruments Laboratory) measured impact forces. Upon activation of the

release mechanism, grains fell vertically and impacted upon the plate, generating measurable seismic waves. To maintain material consistency throughout the experiments, we employed monodisperse glass beads (diameter range: 5 - 30 mm) with uniform material properties (density ρ = 2450 kg/m³, Young's modulus E = 70 GPa, Poisson's ratio ν = 0.2).

Our experimental investigation comprised three distinct test series: single-grain, dual-grain, and multi-grain configurations, with the complete test program summarized in Table 1. In each experiment, grains were released from a hopper positioned 150 mm vertically above the center of the impact plate, ensuring consistent free-fall conditions. The impact dynamics were quantified through multiple measurement techniques. High-speed videography (analyzed using Particle Tracking Velocimetry (PTV) (Ohmi et al., 2000)) provided grain velocity data, while synchronized seismic and force measurements were obtained from the instrumented plate. To ensure statistical reliability, each test condition was replicated three times.

For the multi-grain series, we maintained a constant total mass of 34.6 g across all tests, equivalent to the mass of a single 30 mm diameter grain (d = 30 mm). Grain size distributions (GSDs) in these tests were characterized using two complementary approaches: (1) fractal dimension D_f (Turcotte, 1986) and (2) effective diameters (d_{30}, d_{50}, and d_{94}). The experimental design produced fractal dimensions spanning 0.5 to 4, with monodisperse systems assigned $D_f = 0$ by definition.

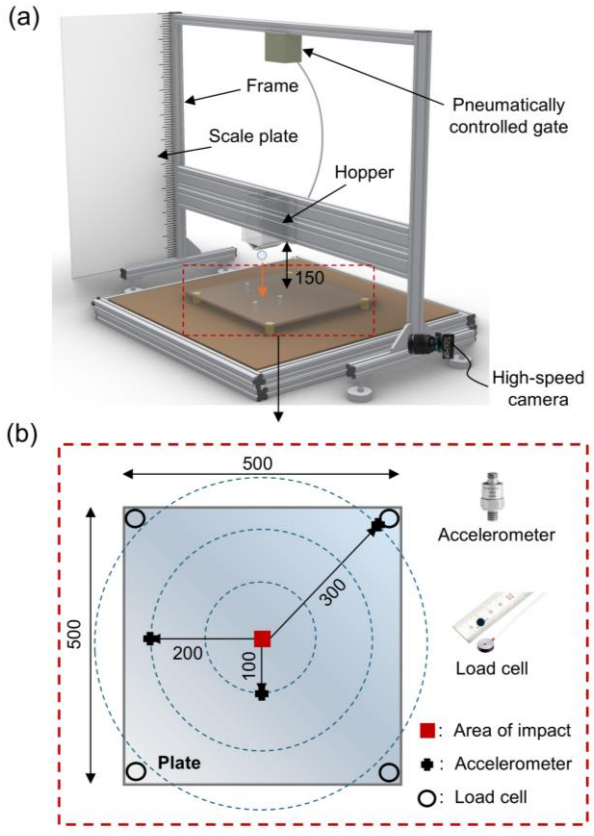

Figure 1. (a) 3D schematic diagram of the experimental setup; (b) plan view of instrumentation layout.

Table 1. Test program[a]

Series	Test ID	Grain diameters (mm)
Single-grained	S1 to S6	5, 10, 16, 20, 25, 30
Dual-grained	D1 to D15	5 + 5, 5 + 10, 5 + 16, 5 + 20, 5 + 25, 10 + 10, 10 + 16, 10 + 20, 10 + 25, 16 + 16, 16 + 20, 16 + 25, 20 + 20, 20 + 25, 25 + 25
Multi-grained (More than two grains)		Grain size distribution: a, b, c, d, e (a, b, c, d, e represents the number of grains with diameters of 5, 10, 16, 20, 25 mm, respectively. The total combined granular mass for each multi-grain test is 34.6 g.)
	M1	0, 3, 0, 3, 0
	M2	1, 3, 2, 0, 1
	M3	3, 3, 0, 1, 1
	M4	5, 2, 4, 1, 0
	M5	6, 2, 2, 2, 0
	M6	4, 6, 5, 0, 0
	M7	6, 10, 2, 1, 0
	M8	13, 1, 4, 1, 0
	M9	5, 10, 4, 0, 0
	M10	0, 19, 0, 1, 0
	M11	8, 26, 0, 0, 0
	M12	42, 2, 1, 0, 1
	M13	43, 6, 0, 0, 1
	M14	53, 8, 3, 0, 0
	M15	55, 8, 1, 1, 0
	M16	54, 12, 2, 0, 0
	M17	64, 3, 0, 2, 0
	M18	55, 16, 1, 0, 0
	M19	56, 20, 0, 0, 0
	M20	216, 0, 0, 0, 0

[a]Each test is repeated three times.

In this study, the vertical components of the seismic signal were exclusively analyzed. For each test, the vertical seismic signal was captured at a sampling frequency of 50,000 Hz, corresponding to a Nyquist frequency of 25,000 Hz. We can extract the representative characteristics from both time domain and frequency domain, as shown in Figure 2.

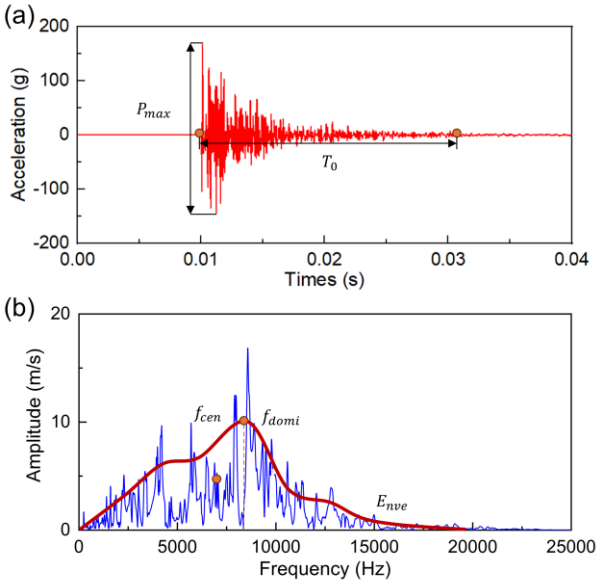

Figure 2. Seismic signal of a typical test in (a) time domain and (b) frequency domain.

The key characteristics that can be extracted from the time-domain signal are as follows:

(1) Peak-peak acceleration P_{max}: The P_{max} is defined as the difference between the maximum and minimum accelerations of the recorded signal: $P_{max} = |a(t)_{max} - a(t)_{min}|$.

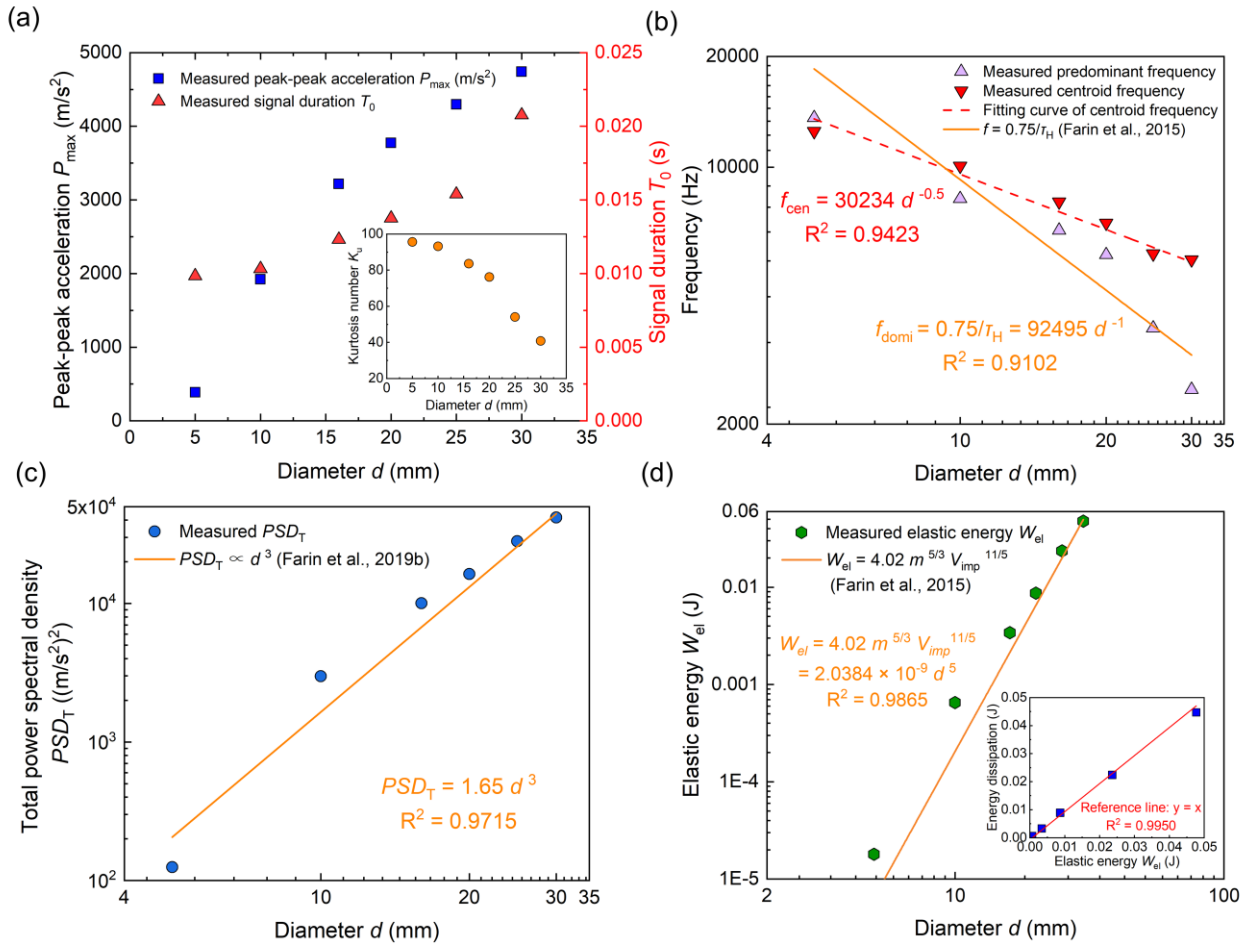

Figure 3. Characteristics of seismic signals induced by single-grain impacts: (a) peak-peak acceleration P_{max} ,kurtosis number K_u and duration T_0) ;b) predominant frequency f_{domi} and centroid frequency f_{cen}) ;c) total power spectral density PSD_T) ;d) elastic energy W_{el}.

(2) Kurtosis number K_u: The K_u quantifies the degree of tailedness or the sharpness of the peak in its probability distribution. K_u is evaluated as: $K_u = \frac{1}{t_T}\int\left(\frac{a(t)-a_{mean}}{S_d}\right)^4 dt$, where S_d is the standard deviation of the seismic signal and t_T is the total sampling time. A high kurtosis indicates that the distribution has heavier tails and a sharper peak compared to a normal distribution.

(3) Signal duration T_0: The duration of the impact moment can be characterized by the effective duration of the seismic signal. According to Lin et al, 2022 and Salo et al, 2018, the duration of the seismic signal is determined by the interval between the 0.05% and 99.95% thresholds of the Husid integral value. Husid integral can be calculated as: $H_u(t) = \int a^2(t)dt$.

The frequency components of elastic waves can be obtained by employing Fast Fourier Transform (FFT) in conjunction with a third-order Butterworth filter. The following characteristics are used to represent the frequency components of the elastic waves:

(1) Predominant frequency f_{domi}: The f_{domi} corresponds to the frequency at which the amplitude reaches its maximum value in the frequency-domain spectrum.

(2) Centroid frequency f_{cen} : The f_{cen} represents the centroid of the frequency spectrum, exhibiting lower sensitivity to variations in the signal-to-noise ratio compared to other frequency characteristics. It provides an indication of the overall frequency level (Lin et al, 2022; Farin et al, 2015). f_{cen} is evaluated as: $f_{cen} = \frac{\int_{f_l}^{f_u}|\tilde{A}(f)|fdf}{\int_{f_l}^{f_u}|\tilde{A}(f)|df}$, where $\tilde{A}(f)$ is the amplitude at frequency f. f_l and f_u represent the lower and upper limits of the frequency filter range, respectively.

(3) Total power spectral density PSD_T: The power spectral density of a signal is a crucial concept that describes the distribution of signal power across different frequencies in the frequency domain. It provides insight into the energy characteristics of the signal (Farin et al., 2019a). The PSD_T can be calculated as: $PSD_T = \int_f PSD(f)df$.

3 EXPERIMENTAL RESULTS

3.1 *Single-Grain Impacts*

The free-fall impacting tests of single grain with six different sizes are regarded as unit tests. The characteristics of the elastic waves in time domain with grain diameter d can be obtained from Figure 3 (a). It is evident that peak-peak acceleration P_{max}, standard deviation S_d and duration T_0 significantly increase with increasing grain size, while kurtosis number K_u markedly decreases linearly as the grain size increases. This indicates that as the grain size grows, the amplitude and the duration of the signals generated by the grains impacting the plate becomes larger, and meanwhile the peaks become less sharp.

Analyzing the characteristics of grains in the frequency domain reveals that the centroid frequency f_{cen} and the

predominant frequency f_{domi} of the signals generated by the impact decrease with increasing grain size, as shown in Figure 3 (b). The centroid frequency and predominant frequency are inversely proportional to $d^{-0.5}$ and to d, respectively. Additionally, it is observed in Figure 3 (c) and (d) that the total power spectral density PSD_T and elastic energy W_{el} is proportional to d^3 and d^5, respectively. So for single-grain tests the relation between the seismic characteristics and the grain diameter is shown as below:

$$f_{cen}(d) = 30234 \times d^{-0.5} \quad (1)$$

$$W_{el}(d) = 2.0384 \times 10^{-9} \times d^5 \quad (2)$$

$$PSD_T(d) = 1.65 \times d^3 \quad (3)$$

3.2 *Dual-Grain Tests Supporting Superposition Principle*

The generation of scattered waves becomes particularly challenging when elastic waves contain broadband frequency components, as they often fail to meet the strict phase-matching conditions required for coherent scattering. In our experiments, the measured signals exhibited a wide frequency spectrum ranging from 200 Hz to 20 kHz. This broadband characteristic suggests that the superposition principle (Koopmann et al., 1989) can be effectively applied to analyze the composite elastic waves generated by multiple grain impacts. According to this principle, the resultant time-domain signal amplitude represents the linear summation of amplitudes produced by individual grain impacts.

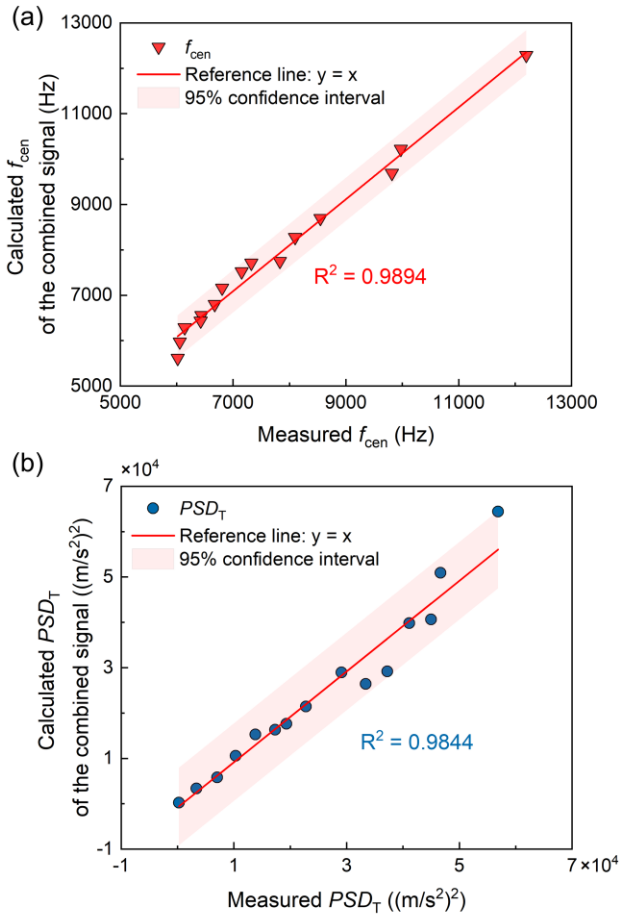

Figure 4. Comparison of seismic signals from experimental measurements and combined signals for dual-grain impacts: (a) centroid frequency f_{cen}; (b) total power spectral density PSD_T.

To verify the applicability of the superposition principle in our experimental context, we performed a systematic validation procedure. Acceleration signals obtained from single-grain impact tests were computationally combined to simulate dual-grain impact signals. Figure 4 presents a comprehensive comparison between the measured dual-grain signals and the combined signals. The analysis reveals excellent agreement between the two datasets, particularly in terms of central frequency (f_{cen}) and total power spectral density (PSD_T). This close correspondence confirms the validity of employing the superposition principle for predicting resultant signals from multiple grain impacts under our experimental conditions.

3.3 *Multi-Grain Tests with Different GSDs*

Figure 5 (a) presents the relationship between elastic energy and three effective grain diameters scatter plot analysis. The data reveals a significant positive correlation between elastic energy and increasing grain size. However, our analysis indicates that while d_{50} and d_{94} may fail to capture critical information about finer grain fractions, d_{30} tends to underrepresent coarser grains. These observations suggest that single-parameter grain size representations are insufficient for fully characterizing grain size distribution (GSD) effects on seismic signal generation.

Figure 5 (b) further demonstrates that both centroid frequency and predominant frequency exhibit consistent trends with respect to the mass-weighted average diameter (d_a), where $d_a = \Sigma(d_i \cdot w_i)$, with d_i representing individual grain sizes and w_i their corresponding mass fractions. Notably, these trends closely mirror those observed in single-grain impact tests, suggesting a strong correlation between d_a and centroid frequency for multi-grain groups with different GSDs.

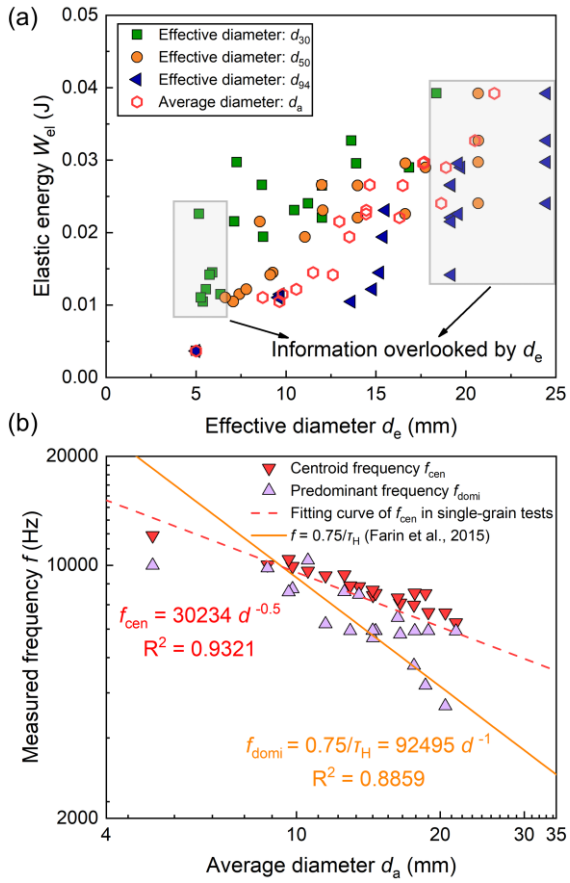

Figure 5. (a) Trends of elastic energy with variations in effective diameter: d_{30}, d_{50}, and d_{94}. (b) trends of centroid frequency and predominant frequency with variations in d_a.

It has been shown that the effective diameters exhibit limited relations with seismic signal characteristics. Here we incorporate D_f along with three effective diameters d_{30}, d_{50}, and d_{94} and perform multiple regression analysis to investigate their relationship with the characteristics of seismic signals. Then we introduce a newly-proposed GSD parameter GSD_e, which more effectively accounts for the size distribution of the grains:

$$GSD_e = d_{30} \cdot {D_f}^{1/6} \quad (4)$$

All characteristics demonstrate strong linear correlations, with correlation coefficients exceeding 0.85. The relationships are expressed by the following equations:

$$f_{cen} = -6665.5 \lg(GSD_e) + 15168.16 \quad (5)$$

$$W_{el} = 0.0415 \lg(GSD_e) - 0.0186 \quad (6)$$

$$PSD_T = 56551.92 \lg(GSD_e) - 5792.32 \quad (7)$$

These trends demonstrate a strong correlation between GSD_e and the seismic signal. Furthermore, GSD_e provides enhanced characterization of GSDs by incorporating both effective diameters and fractal dimension, enabling more accurate inversion related to seismic signals.

4 CONCLUSIONS

This study systematically examines the correlation between grain size distribution (GSD) and impact-induced seismic signals through controlled free-fall experiments. The principal findings can be summarized as follows:

(1) Our results demonstrate substantial variation in seismic signal characteristics across different GSDs. We introduce a novel composite parameter, GSD_e, that integrates fractal dimension (D_f) with conventional grain size metrics. This parameter shows statistically significant correlations with three fundamental seismic parameters: centroid frequency (f_{cen}), elastic energy (W_{el}), and total power spectral density (PSD_T). The strong predictive capability of GSD_e suggests its potential for field applications where seismic monitoring could serve as a proxy for GSD characterization in natural granular flows.

(2) Single-grain impact tests reveal distinct scaling relationships between grain diameter d and seismic parameters: $f_{cen} \propto d^{-0.5}$, $W_{el} \propto d^5$, and $PSD_T \propto d^3$. Furthermore, dual-grain experiments confirm the linear superposition principle holds for impact-generated seismic waves. These empirical relationships provide a physical basis for modeling seismic signals in polydisperse granular flows, significantly improving our ability to interpret seismic data from natural geohazards such as rockfalls and debris flows.

Future work will involve comprehensive theoretical refinement and experimental validation of the seismic physical model through controlled flume testing. In this study, the effects of shear and sliding processes that occur during mass movement, which can also contribute significantly to the seismic response, have not been considered. Additionally, our experiments are conducted at a laboratory scale, and future work should focus on upscaling to more realistic field conditions. Furthermore, this study focuses exclusively on dry grains, while the inclusion of water-saturated sands and clays is necessary to extend the applicability of the seismic impact model to a broader range of natural scenarios. Further research is required to address these limitations and advance the understanding of seismic signals generated by granular geohazards.

5 ACKNOWLEDGEMENTS

The work described in this paper was fully supported by a grant from the Research Grants Council of the Hong Kong Special Administrative Region, China (Project No. C7085-24G_ CRF 2024/25) and the National Natural Science Foundation of China (42120104002).

6 REFERENCES

Barrière, J., Krein, A., Oth, A., & Schenkluhn, R. 2015. An advanced signal processing technique for deriving grain size information of bedload transport from impact plate vibration measurements. Earth Surface Processes and Landforms, 40(7), 913–924.

Dammeier, F., Moore, J. R., Haslinger, F., & Loew, S. 2011. Characterization of alpine rockslides using statistical analysis of seismic signals. Journal of Geophysical Research, 116(F4), F04024.

De Haas, T., Åberg, A. S., Walter, F., & Zhang, Z. 2021. Deciphering seismic and normal-force fluctuation signatures of debris flows: An experimental assessment of effects of flow composition and dynamics. Earth Surface Processes and Landforms, 46(11), 2195–2210.

Farin, M., Mangeney, A., De Rosny, J., Toussaint, R., & Trinh, P. 2019. Relations Between the Characteristics of Granular Column Collapses and Resultant High-Frequency Seismic Signals. Journal of Geophysical Research: Earth Surface, 124(12), 2987–3021.

Farin, M., Mangeney, A., Toussaint, R., Rosny, J. D., Shapiro, N., Dewez, T., Hibert, C., Mathon, C., Sedan, O., & Berger, F. 2015. Characterization of rockfalls from seismic signal: Insights from laboratory experiments. Journal of Geophysical Research: Solid Earth, 120(10), 7102–7137.

Farin, M., Tsai, V. C., Lamb, M. P., & Allstadt, K. E. 2019. A physical model of the high-frequency seismic signal generated by debris flows. Earth Surface Processes and Landforms, 44(13), 2529–2543.

Hu, W., Hicher, P.-Y., Scaringi, G., Xu, Q., Van Asch, T. W. J., & Wang, G. 2018. Seismic precursor to instability induced by internal erosion in loose granular slopes. Géotechnique, 68(11), 989–1001.

Iverson, R. M. 1997. The physics of debris flows. Reviews of Geophysics, 35(3), 245–296.

Kim, B. C., & Lowe, D. R. 2004. Depositional processes of the gravelly debris flow deposits, South Dolomite alluvial fan, Owens Valley, California. Geosciences Journal, 8(2), 153–170.

Koopmann, G. H., Song, L., & Fahnline, J. B. 1989. A method for computing acoustic fields based on the principle of wave superposition. The Journal of the Acoustical Society of America, 86(6), 2433–2438.

Le Roy, G., Helmstetter, A., Amitrano, D., Guyoton, F., & Le Roux-Mallouf, R. 2019. Seismic Analysis of the Detachment and Impact Phases of a Rockfall and Application for Estimating Rockfall Volume and Free-Fall Height. Journal of Geophysical Research: Earth Surface, 124(11), 2602–2622.

Li, T., Wang, Y., Cheng, Q., Lin, Q., Shi, A., Ming, J., & Luo, X. 2024. Experiments on Landquakes Generated by Free-Falling Granular Masses: Implications for Rockfall Impact Dynamics. Earth and Space Science, 11(6), e2023EA003402.

Lin, Q., Wang, Y., Cheng, Q., Deng, K., Liu, S., & Li, K. 2022. Characteristics of the Seismic Signal Generated by Fragmental Rockfalls: Insight From Laboratory Experiments. Journal of Geophysical Research: Solid Earth, 127(11), e2022JB025096.

Ohmi, K., & Li, H.-Y. 2000. Particle-tracking velocimetry with new algorithms. Measurement Science and Technology, 11(6), 603–616.

Saló, L., Corominas, J., Lantada, N., Matas, G., Prades, A., & Ruiz-Carulla, R. 2018. Seismic Energy Analysis as Generated by Impact and Fragmentation of Single-Block Experimental Rockfalls. Journal of Geophysical Research: Earth Surface, 123(6), 1450–1478.

Schimmel, A., & Hübl, J. 2016. Automatic detection of debris flows and debris floods based on a combination of infrasound and seismic signals. Landslides, 13(5), 1181–1196.

Song, P., & Choi, C. E. 2021. Revealing the Importance of Capillary and Collisional Stresses on Soil Bed Erosion Induced by Debris Flows. Journal of Geophysical Research: Earth Surface, 126(5), e2020JF005930.

Turcotte, D. L. 1986. Fractals and fragmentation. Journal of Geophysical Research: Solid Earth, 91(B2), 1921–1926.
Wyss, C. R., Rickenmann, D., Fritschi, B., Turowski, J. M., Weitbrecht, V., & Boes, R. M. 2016. Laboratory flume experiments with the Swiss plate geophone bed load monitoring system: 1. Impulse counts and particle size identification: flume experiments with the swiss plate geophone: methodology. Water Resources Research, 52(10), 7744–7759.